

Smart Ankleband for Plug-and-Play Hand-Prosthetic Control

Dean Zadok¹, Oren Salzman¹, Alon Wolf² and Alex M. Bronstein¹

Abstract—Building robotic prostheses requires the creation of a sensor-based interface designed to provide the robotic hand with the control required to perform hand gestures. Traditional Electromyography (EMG) based prosthetics and emerging alternatives often face limitations such as muscle-activation limitations, high cost, and complex-calibration procedures. In this paper, we present a low-cost robotic system composed of a smart ankleband for intuitive, calibration-free control of a robotic hand, and a robotic prosthetic hand that executes actions corresponding to leg gestures. The ankleband integrates an Inertial Measurement Unit (IMU) sensor with a lightweight temporal neural network to infer user-intended leg gestures from motion data. Our system represents a significant step towards higher adoption rates of robotic prostheses among arm amputees, as it enables one to operate a prosthetic hand using a low-cost, low-power, and calibration-free solution. To evaluate our work, we collected data from 10 subjects and tested our prototype ankleband with a robotic hand on an individual with upper-limb amputations. Our results demonstrate that this system empowers users to perform daily tasks more efficiently, requiring few compensatory movements.

I. INTRODUCTION

People with upper-limb differences in general and upper-limb amputations in particular face significant challenges in regaining functional independence, often struggling with Activities of Daily Living (ADLs) [1] such as dining, dressing, and participating in work or social activities. Despite the clear need, current-upper limb prosthetics often lack sufficient functionality, intuitive control and may cause discomfort or pain. EMG has been a dominant technology in prosthetic-arm control for decades, relying on sensors to detect electrical activity in the muscles of the residual limb. However, these solutions come with several limitations. The inability to activate muscles years after misuse, the challenges posed by neurological or phantom pain, and the complex training required, all contribute to low adoption rates among amputees [2], [3]. This lack of reliable and user-friendly solutions can lead to frustration, decreased quality of life, and reluctance to experiment with newer prosthetics.

In recent years, researchers have begun to look for alternative approaches to provide prosthetic arms with control procedures that do not involve muscle activation. Available solutions involve autonomous behavior, such as predicting the action type using motion [4], [5], detecting objects through vision sensing [6], [7], or instructing the hand using voice control [8]. In addition, brain-computer interfaces (BCIs) offer to enable the control of robotic devices through the



Fig. 1: Our robotic system is comprised of two components: C1 smart ankleband (left) and C2 robotic hand (right). An IMU placed in the smart ankleband collects and stores signals in a buffer which serves as an input to a machine-learning model able to classify user leg gestures. The corresponding action is transmitted to the robotic hand.

interpretation of brain activity via electroencephalography (EEG) [9]. Such methods include various operational limitations. For example, environmental factors such as lighting and motion may degrade the precision of vision-based methods, and to process high-resolution images or sound, one will need to install expensive wearable hardware to allow precise prosthetic control. Addressing these limitations, including the discomfort associated with muscle-based control, is crucial for increasing the adoption of robotic prosthetic arms.

In response to these challenges, we present a low-cost, simple and effective approach to interface and control a robotic prosthetic hand for upper-extremity amputations. Our system (Fig. 1) is based on a smart ankleband, composed of a lightweight microcontroller, a battery, and an IMU. The ankleband uses a pre-trained machine-learning model to infer leg gestures that the user performs, which correspond to predefined actions, given the motion data generated from the IMU. These are then transmitted to the robotic hand using a wireless interface which, in turn, executes the relevant action.

The core contribution of this paper is an end-to-end low budget low power wearable system that allows to seamlessly control a robotic hand, calibration-free.¹ Our success stems from the design choices we took to construct the entire

¹Department of Computer Science, Technion, Haifa, Israel {deanzadok,osalzman,bron}@cs.technion.ac.il

²Department of Mechanical Engineering, Technion, Haifa, Israel alonw@me.technion.ac.il

¹Our code and dataset are publicly available at <https://github.com/deanzadok/ankleband>.

system: (i) The development of a comfortable and universally wearable ankleband to be worn by any person, (ii) employing a lightweight machine-learning model and implementing it specifically for low-budget hardware, and (iii) a fully standalone setup designed to work as a “plug-and-play” system and does not require additional hardware or calibration for daily use. In our empirical evaluation, we demonstrate the ability of our system to accurately infer gestures for unseen individuals, by collecting data from 10 subjects. Finally, we demonstrate via a user study in the lab how the system can be used by a user with an upper-limb amputation and enhance the performance of ADL.

II. RELATED WORK

The most common way to provide control is using surface electromyography (sEMG) [10], [11], [12]. In this setting, the subject usually wears an armband equipped with electrodes that detect electric potential. A high number of electrodes allows differentiation between a large number of predefined gestures. Additionally, researchers investigated alternative approaches, such as using ultrasound (US) to infer muscle dynamics and improve detection of finer finger motions [13], [14]. Unfortunately, subjects tend to neglect the use of such muscle-based prosthetic hands due to several reasons. Among them are continuous pain of activating residual muscles, or an inconvenience of using sensors that require calibration and stable placement.

Recently, alternative approaches have emerged that leverage autonomy or easier and more intuitive control of robotic hands toward improving adoption rates of prosthetic hands. Researchers proposed solutions that are easier to operate and do not require calibration, such as activating a prosthetic hand using voice control [8], or using EEG to provide control without the involvement of the peripheral nervous system [9]. In addition, recent studies explore the idea of activating leg muscles to provide upper-limb prosthetic control. Popular examples include the installation of EMG sensing to detect leg lower-limb muscle activity instead of upper-limb muscles [15]. More affordable solutions were proposed to detect leg motions. For example, providing an electronic insole with a push-button [16], using a camera to detect foot gestures [17], and using vision sensing to provide autonomous control for robotic hands [6], [7]. Moreover, recent studies demonstrated that leg gestures can be used to personalize control for prosthetic arms [18], but the question of how accurately we can create a generalizable system for a wide range of subjects remained unanswered.

In this work, we focus on the applicability of using a mobile and data-driven solution to detect leg gestures in real time. We are motivated by previous successes in applying machine-learning techniques for various applications involving human activity. To enhance the treatment of patients, researchers showed how to enhance Parkinson’s treatment using motion detection [19], or providing feedback during rehabilitation exercises of shoulder pain [20]. In rehabilitation engineering, researchers showed recognition of exoskeleton activity [21], remote control of a television [22], and even

instructing a robotic manipulator using human motions [23]. These works and additional papers suggest that machine learning (ML) techniques have the potential to recognize complex gestures in real time [24], [25], [26].

III. SYSTEM DESIGN

A. Overview

Our design choices are guided by three primary objectives aimed at increasing the adoption rates of assistive devices among upper-limb amputees:

- O1** Affordability—the system cost should be minimized as this is a significant barrier to adoption.
- O2** Reliability—the system should exhibit high performance even under low-energy and cost constraints.
- O3** User independent—the system should be “plug and play” eliminating the need for extensive calibration or additional data collection for new users.

To this end, we propose a robotic system (Fig. 1) consisting of two components: **C1** A wearable device placed on the ankle referred to as the *smart ankleband* and **C2** a robotic hand. The smart ankleband is tasked with detecting intended leg gestures performed by the user and transmitting them to the robotic hand using a wireless interface which, in turn, executes the action corresponding to the performed gesture.

Consequently, the smart ankleband (Fig. 1, left and Fig. 3) includes an IMU motion sensor for motion detection, a microcontroller for leg gesture classification and command transmission using Bluetooth Low-Energy (BLE) communication and a power source. Regarding the robotic hand (Fig. 1, right), our system is generic and can support a wide range of platforms. We chose a robotic hand based on an open-source project designed to make such devices accessible as well as programmable².

In terms of functionality, following participants feedback, we define four actions to be executed by the robotic hand: grasp, point, rotate wrist left and rotate wrist right (Fig. 2). Accordingly, we define four different leg gestures corresponding to each action. To return to an open-hand state, the user should perform the last-performed gesture. Importantly, the specific leg gestures were selected based on the spatial displacement of the IMU sensor, with the four distinct gestures designed to simplify the classification process (Fig. 2). While the gestures are similar to those used in previous papers adopting leg-gesture classification algorithms [18], we require that each gesture must be performed twice to minimize unintended activations.

B. Smart-Ankleband Physical Design

Recall that the smart ankleband contains a microcontroller, an IMU, and a power source. These are integrated into a comfortable and compact wearable design (Fig. 3). There is no need for additional clothing or user-specific adaptations. To increase user comfort, the microcontroller and IMU are

²Full details on how to rebuild and program the hand are in <https://github.com/Haifa3D/hand-mechanical-design>.

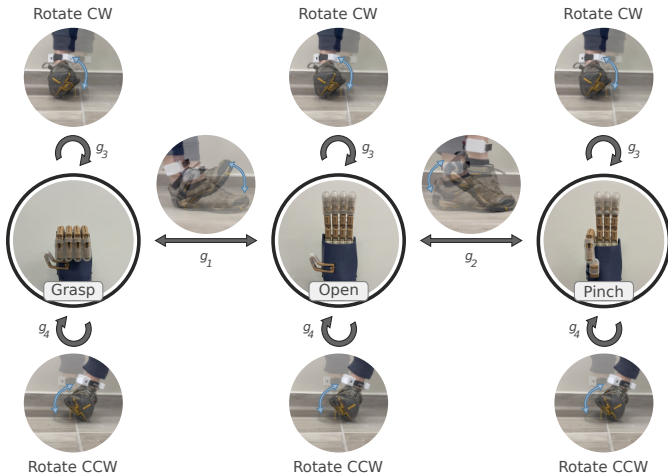


Fig. 2: State machine depicting leg gestures and corresponding hand actions. We start with an open hand, and the user can either grasp (leg gesture g_1), or pinch (leg gesture g_2). To rotate the hand clockwise (CW) or counterclockwise (CCW), the user can use leg gestures g_3 or g_4 , respectively. Rotation is available regardless of the state.

housed in one component while the power source is housed in a second one maximizing weight distribution.

To allow for low cost (**O1**) while ensuring reliability (**O2**), we selected the ESP32 microcontroller for its balance of processing power, varied interfaces, and energy efficiency and the Adafruit BNO08X IMU for its cost-effectiveness and ability to generate high-frequency 3D acceleration and angular velocity data, essential for accurate gesture recognition. Specifically, the IMU provides data at a rate of up to 1 kHz. Finally, the power source is a 3.7V battery with 950 mAh. The overall cost of the smart ankleband is estimated at 30 USD and can be built with standard 3D printing capabilities and basic soldering tools.

C. Leg-Gesture Classification

Recall that we predefine a set of leg gestures used by the user to control the robotic hand which are identified using the IMU. Specifically at time t the IMU outputs a vector $x_t = [\ddot{x}_t, \ddot{y}_t, \ddot{z}_t, \dot{\theta}_t^x, \dot{\theta}_t^y, \dot{\theta}_t^z]$. Here, $\ddot{x}_t, \ddot{y}_t, \ddot{z}_t$ are the accelerations in the x , y , and z axes, and $\dot{\theta}_t^x, \dot{\theta}_t^y, \dot{\theta}_t^z$ are the roll, pitch, and yaw angular velocities. The input \bar{x}_t to our classifier is a sequence of k consecutive IMU signals recorded between times t and $t+k-1$.³ Namely $\bar{x}_t := \langle x_t, \dots, x_{t+k-1} \rangle$. The output p_t of our classifier is a vector of gesture probabilities at time t . Specifically, $p_t := \langle p_t^0, \dots, p_t^4 \rangle$, where p_t^0 is the probability for no gesture and p_t^i for $i \in \{1, \dots, 4\}$ represents the probability of gesture g_i being performed at time t .

As the user can perform a leg gesture at any given time and its length varies, we need to carefully associate the input \bar{x}_t to our classifier and the continuous time interval $[t_s^g, t_e^g]$

³The value k is a hyper parameter discussed in Sec. IV. It should be large enough to capture leg gestures which typically take between 0.5 to 1 seconds but small enough to be processed by our lightweight microprocessor as well include at most one leg gesture.



Fig. 3: Physical layout of the smart ankleband. The front section contains the microcontroller and IMU sensor, and the rear section contains a battery for a day-long use.

duration during which leg gesture g was performed. Now, we say that leg gesture g is fully present within input sequence \bar{x}_t if $t \leq t_s^g$ and $t_e^g \leq t+k-1$. To this end, given time interval $[t_s^g, t_e^g]$ for leg gesture g and input sequence \bar{x}_t , we denote their Jaccard index by σ . Namely,

$$\sigma := \frac{[t_s^g, t_e^g] \cap [t, t+k-1]}{[t_s^g, t_e^g] \cup [t, t+k-1]}. \quad (1)$$

This threshold was chosen empirically and we elaborate on how it was found in Sec. IV-C. Our classifier is a compact neural network includes a 1D convolutional layer for temporal feature extraction from the 6-dimensional IMU signal, followed by batch normalization to enhance performance for unseen users, and a multi-layer perceptron to generate the gesture probability vector p_t . Further details on the training process and real-time inference can be found in Sec. IV-B.

IV. EVALUATION

In this section, we evaluate our approach for classifying leg gestures under computation constraints, in addition to the evaluation of the smart ankleband as a robotic system in real time. We start (Sec. IV-A and IV-B) by describing our experimental setup, data collection, and training methodology. We then analyze our chosen model as part of an ablation study (Sec. IV-C) and finish with real-time experiments on a participant with lower-arm amputation (Sec. IV-D).

A. Setup and Data Collection

We collected data from 10 subjects; averaging at 27 years old, five of whom are men and five of whom are women. During data collection, the frequency of the IMU sensor was set to 200 Hz, and a Vicon motion-capture system was used to monitor the motion of the foot to compute label intervals after the recordings. All subjects wore the smart ankleband on their right leg and were confirmed to be right-footed and without any neurological disorders or conditions in their legs.

Subjects were instructed to repeatedly perform each gesture for one or two minutes, depending on their performance. In addition, subjects were asked to behave naturally for an additional period of two minutes to collect data that will serve as noise, or no leg gesture, for accurate model training. We repeated this process two times. In the first time, subjects were instructed to sit in a chair and perform the aforementioned process. In the second time, subjects were instructed to repeat the entire process while standing. In total,

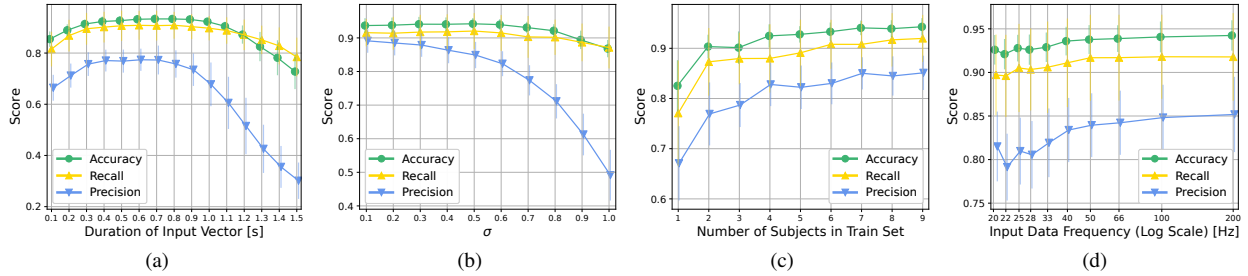


Fig. 4: (a) Performance as a function of the duration of the input vector in seconds. (b) Performance as a function of σ (the minimum percentage of gesture overlap with the input window, Sec. III-C). (c) Performance as a function of the number of subjects in the training set. (d) Performance as a function of the sampling frequency of the IMU sensor. All experiments are averaged over 10 folds, with one subject left out for test set in each fold. Vertical segments denote one standard deviation.

for each subject we recorded 8-16 labeled leg gestures and four additional minutes of regular activity. The process was approved by the institution’s Ethics Committee. The final dataset includes a total of 2.5 million x_t samples. For each sample, we create the input vector \bar{x}_t and label it to receive the tuple $\langle \bar{x}_t, p_t \rangle$ defined in Sec. III-C.

B. Model Training and Inference

Before training, accelerations $\ddot{x}_t, \ddot{y}_t, \ddot{z}_t$ and angular velocities $\dot{\theta}_t^x, \dot{\theta}_t^y, \dot{\theta}_t^z$ were normalized to (approximately) fit the range of $[-1, 1]$ by dividing each one using the constants $c_a = 10$ and $c_g = 2$, respectively⁴. On feedforward, our model receives a sequence of $k = 60$ IMU samples \bar{x}_t , such that each sample is normalized and fed to the network. To ensure balanced class distribution within training batches, weighted sampling was employed. On backpropagation, for the predicted classes probabilities, the loss function for $N = 128$ samples in each batch is the Cross-Entropy Loss, i.e., $\mathcal{L}_{CE} = \sum_{j=1}^N \sum_{i=1}^5 [-g_i \log(p_{j,g_i})]$ where p_{j,g_i} is the predicted probability that sample j belongs to leg gesture g_i . All training sessions were executed for 50 epochs, to avoid overfitting. Adam [27] was used as the optimization method, with a learning rate of 0.0001.

For real-time inference, the model was implemented using Eigen in C++, and model weights were extracted from the training procedure and uploaded as constant data arrays to the ESP32 microcontroller. The frequency of model execution during runtime on the ESP32 is approximately 75 Hz.

C. Model Study

Here, we present experiments and insights related to the design (e.g., what machine-learning classifier to use) and performance (e.g., what hyper-parameter to choose) of our leg-gesture classifier. In all experiments, we evaluated the models using 10-fold cross-validation which simulates a scenario where we test the model on a new user who did not participate in our data-collection procedure. Specifically, for each evaluation, the dataset was divided into 10 folds,

each containing data from a specific subject. The i ’th subject was set aside for testing and not used in training, while the remaining nine folds were used for training. This process simulates a scenario where we test the model on a new user who did not participate in our data collection procedure.

What is the duration for the input window? Recall (Sec. IV-B) that our classifier receives as input a vector \bar{x} of k IMU signals. Vector \bar{x} should capture a leg gesture whose average duration is estimated to be between 0.5 and 1 seconds. Thus, we evaluated the performance of our model for different durations of \bar{x} , ranging from 0.1 to 1.5 seconds (Fig. 4a). Performance (measured in accuracy, recall and precision) is best using an an input duration between 0.6 to 0.8 seconds. When factoring in memory constraints, which limit the size of the tensors during inference, we set our sensor to a frequency of 100 Hz and chose the duration to be 0.6 seconds, resulting in $k = 60$ IMU samples.

How should we determine the existence of labels in input windows? The second hyperparameter we optimized for was the threshold σ determining whether a leg gesture that partially exists in the input window should be labeled as present or not (Eq. (1)). Here, we evaluated σ values between 0.1 and 1.0 (Fig. 4b). Interestingly, higher values of σ lead to a significant decrease in performance, particularly in precision values and one should choose a relatively low value of σ . However, to ensure that each input window contains only one prominent gesture to be identified, we must ensure that $\sigma \geq 0.5$. Thus, we set $\sigma = 0.5$.

How many subjects are required for the model to understand the gestures of an unseen subject? Recall that one of the primary objectives of the system design is that it should be “plug-and-play” (O3, Sec. III). To this end, we evaluated the number of subjects needed to train a model such that is seamlessly generalizes to new users. For each evaluation, we trained the model while leaving out one subject for a test set, and randomly selecting subjects for training from the remaining nine subjects. The results (Fig. 4c) indicate that we require only one subject in the training process to detect at least 75% of the gestures performed by the unseen subject (see recall values). More importantly, the performance improves significantly with the

⁴The normalization factor for acceleration is higher due to the existence of gravity measurements, which means that at rest, the size of the 3D acceleration vector is approximately 9.81.

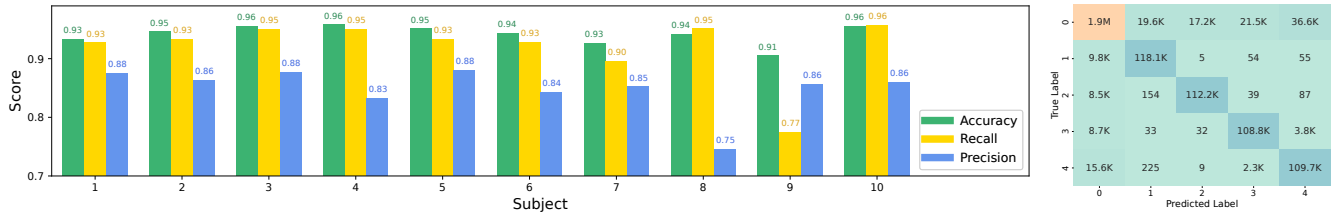


Fig. 5: Performance across subjects and gestures. (Left) Metrics for all ten subjects, plotted using leave-one-subject-out cross-validation. (Right) Confusion matrix for the five classes: a no-gesture class and the four gestures. Rows and columns represent true labels and predictions, respectively. Results show that misidentifying gestures as other gestures is negligible.

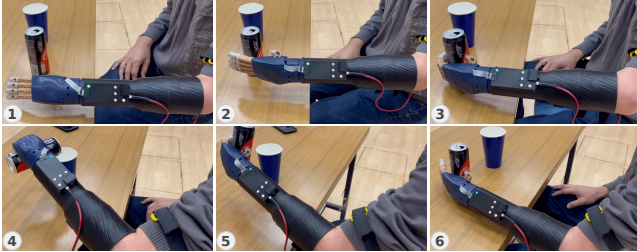


Fig. 6: A representative example of using our smart ankleband with the robotic hand to perform a daily activity. The user reaches to the soda can (1) and grasps it using leg gesture g_1 (2 and 3). Then, the user lifts and rotates CW using leg gesture g_3 to pour the beverage (4). Finally, the user rotates CCW using g_4 (5) and opens the hand using g_1 to leave the soda can on the table (6).

addition of the second subject and gradually with the addition of more subjects. These findings suggest that we can indeed achieve sufficient performance with a relatively small dataset, making it practical for real-world deployment.

How important is it for our system to work under high frequency? The frequency used by our model during inference induces a trade-off between reducing the data resolution for faster inference and memory efficiency, and preserving the quality of the input data for potentially better performance. Moreover, high-quality performance under a low frequency would allow to choose cheaper hardware (see Sec. III-B). Thus, we plotted the performance of our model for input frequencies ranging from 20 Hz to 200 Hz. Results, summarized in Fig. 4d, show that the model improves gradually as the frequency increases. Thus, we set the highest frequency that fits our hardware, which was 100 Hz.

How affected are the results by the specific subject and the specific leg gestures chosen for this task? We plotted the different metrics for each subject individually to see how efficient the model is across different subjects (Fig. 5, left). The results show that the model achieved exceptional performance for the majority of the subjects. However, we observed that when testing the model for subject #9, the model had difficulties in detecting gesture g_4 . We associate this gap in performance to the smaller magnitude of motion performed by this subject for this specific gesture, who had limited ability to flex the ankle. Overall, the method works

for all subjects, highlighting the potential for large-scale adoption of our smart ankleband.

Additionally, we plotted the confusion matrix of the entire dataset to see how the model classifies each gesture compared to the ground truth. The results show that gesture g_4 was the most challenging for the model to recognize, but overall, the model is generally effective in predicting all four gestures. Importantly, it can be seen that the model can avoid misclassifying gestures as other gestures, ensuring safety when performing tasks that require accurate and reliable gesture recognition. Moreover, the only gestures that can be misclassified are g_3 and g_4 which correspond to twisting the ankle left and right, respectively. However, even this happens a negligible amount of times

Can we use alternative models? The modular design of our system allows to substitute several components, including the classifier. Previous studies used larger deep-learning (DL) models [4], [5], but these are not feasible for our system due to its limited hardware resources. Given our hardware constraints, we evaluated classical data-driven approaches known to be effective for similar tasks while also having a low memory footprint compared to DL methods. One such approach is to perform feature extraction following by a classification algorithm over the extracted feature. We experimented with Dynamic Time Warping (DTW) [23], [28] for feature extraction followed by either Linear Discriminant Analysis (LDA) [29] or Support Vector Machine (SVM) [18], [23], to perform gesture recognition. Unfortunately, the accuracy of these classical approaches was lower than DL models when applied to our data. A possible explanation is that unlike high-end sensors, our IMU sensor produces noisy data, requiring a de-noising step which DL methods excel at [30], [31]. Furthermore, we implemented alternative optimization techniques, such as domain adaptation [32] and contrastive learning [33], [34], to improve generalization to unseen subjects. However, these techniques did not outperform the supervised-learning approach which proved to be the ultimate choice in our setting.

D. Robotic System Study

To evaluate our system in ADL, we conducted a user study in the lab with a participant who had a transradial amputation of his left hand. The participant has undergone amputation 12 years prior to the study, and is experienced with prosthetic



Fig. 7: Examples of tasks completed as part of the AM-ULA test. Starting from the top left and moving clockwise: pushing a door knob, hammering a nail, writing on a blank paper, and folding a towel.

devices. The experiment consisted of two tests: First, the participant performed each gesture ten times without the robotic hand in order to experiment with the smart ankleband. Then, the participant completed the “Activities Measure for Upper-limb Amputees” (AM-ULA) test [35], which involves using the prosthetic device to perform 18 listed activities, such as folding a towel, dialing with a mobile phone, or pouring a beverage (Fig. 6 and 7). This test evaluates not only the functionality of our ankleband but also the user’s proficiency and interaction with the robotic system.

In the first part (experimenting with the smart ankleband) we validated that this was indeed the first time the participant had worn the smart ankleband. Afterwards, we measure the success rate to perform each leg gesture: The participant successfully performed 9 out of 10 repetitions for the first leg gesture, and 10 out of 10 for the other three, demonstrating how intuitive-to-use the smart ankleband is and how it requires minimal training. In the second part (the AM-ULA test), we turned on the robotic hand and ensured that the smart ankleband was connected. We then instructed the participant to perform the 18 tasks, encouraging to use the robotic hand naturally. The test revealed that the participant used grasp and pinch actions almost equally, with a total of 34 grasp and 32 pinch intentions, and only three instances of wrist rotation. The end-to-end system executed 78% of the intentions, with no misclassifications between gestures. We associate the difference in the error rates between this experiment and the offline experiment (Fig. 5) to communication malfunctions with the robotic hand that occurred during the experiment. Notably, throughout the two-hour experiment, our ankleband operated reliably and misclassified native movements as gestures only four times, showing promising performance for ADL.

V. DISCUSSION & FUTURE WORK

In this paper, we presented a robotic system to operate a robotic prosthetic arm using a smart ankleband that detects intended ankle gestures. We show how our system can be

used as a “plug-and-play” system by wearing the ankleband and the robotic hand, and performing ADL seamlessly and without the need for prolonged personalization procedures. Our results show that subject generalization is accessible under hardware constraints (with recall above 90%) and that it is not needed to perform large-scale data collection to achieve a reliable and user-independent system (Fig. 4c).

Future directions we are exploring include (i) Performing a large-scale study to utilize the modularity of our system: This may include exploring alternative options of input gestures, or interesting application interfaces that can use our system. (ii) Developing a smart ankleband that can proportionally control digital or robotic devices: This can be useful in terms of applications in which users with disabilities are unable to perform continuous motions with their hands. (iii) Extending our system to perform typing motions: Recent advancements on robotic prostheses demonstrated promising performance on restoring dexterous finger control [14] and here we are interested with enabling users with disabilities with the full capabilities required to operate digital devices.

REFERENCES

- [1] P. F. Edemekong, D. Bomgaars, S. Sukumaran, and S. B. Levy, “Activities of daily living,” 2019.
- [2] E. A. Biddiss and T. T. Chau, “Upper limb prosthesis use and abandonment: a survey of the last 25 years,” *Prosthet. Orthot. Int.*, vol. 31, no. 3, pp. 236–257, 2007.
- [3] L. C. Smail, C. Neal, C. Wilkins, and T. L. Packham, “Comfort and function remain key factors in upper limb prosthetic abandonment: findings of a scoping review,” *Disabil. Rehabil.: Assist. Technol.*, vol. 16, no. 8, pp. 821–830, 2021.
- [4] C. Uyanik, S. F. Hussaini, E. Erdemir, E. Kaplanoglu, and A. Sekmen, “A deep learning approach for final grasping state determination from motion trajectory of a prosthetic hand,” *Procedia Comput. Sci.*, vol. 158, pp. 19–26, 2019.
- [5] J. Cui, Z. Li, H. Du, B. Yan, and P. Lu, “Recognition of upper limb action intention based on IMU,” *Sensors*, vol. 22, no. 5, p. 1954, 2022.
- [6] M. N. Castro and S. Dosen, “Continuous semi-autonomous prosthesis control using a depth sensor on the hand,” *Front. neurorobot.*, vol. 16, p. 814973, 2022.
- [7] M. A. B. Sarker, J. P. S. Sola, A. Jones, E. Laing, E. Sola-Thomas, and M. H. Imtiaz, “Vision controlled sensorized prosthetic hand,” *arXiv*, vol. abs/2407.12807, 2024.
- [8] M. H. Asyali, M. Yilmaz, M. Tokmakci, K. Sedef, B. H. Aksebzeci, and R. Mittal, “Design and implementation of a voice-controlled prosthetic hand,” *Turk. J. Electr. Eng. Comput. Sci.*, vol. 19, no. 1, pp. 33–46, 2011.
- [9] P. C. Maibam, D. Pei, P. Olikkal, R. K. Vinjamuri, and N. M. Kakoty, “Enhancing prosthetic hand control: A synergistic multi-channel electroencephalogram,” *Wearable Technologies*, vol. 5, p. e18, 2024.
- [10] W. Li, P. Shi, and H. Yu, “Gesture recognition using surface electromyography and deep learning for prostheses hand: state-of-the-art, challenges, and future,” *Frontiers in neuroscience*, vol. 15, p. 621885, 2021.
- [11] U. Côté-Allard, C. L. Fall, A. Drouin, A. Campeau-Lecours, C. Gosselin, K. Glette, F. Laviolette, and B. Gosselin, “Deep learning for electromyographic hand gesture signal classification by leveraging transfer learning,” *arXiv*, vol. abs/1801.07756, 2018.
- [12] R. C. Sîmpetru, M. März, and A. D. Vecchio, “Proportional and simultaneous real-time control of the full human hand from high-density electromyography,” *IEEE Trans. Neural Syst. Rehabilitation Eng.*, 2023.
- [13] J. McIntosh, A. Marzo, M. Fraser, and C. Phillips, “Echoflex: Hand gesture recognition using ultrasound imaging,” in *CHI*, 2017, pp. 1923–1934.
- [14] D. Zadok, O. Salzman, A. Wolf, and A. M. Bronstein, “Towards predicting fine finger motions from ultrasound images via kinematic representation,” in *ICRA*, 2023, pp. 12 645–12 651.

- [15] C. Lin, Y. Tang, Y. Zhou, K. Zhang, Z. Fan, Y. Yang, Y. Leng, and C. Fu, "Foot gesture recognition with flexible high-density device based on convolutional neural network," in *IEEE ICARM*, 2021, pp. 306–311.
- [16] P. L. Bishay, J. Wilgus, R. Chen, D. Valenzuela, V. Medina, C. Tan, T. Ittner, M. Caldera, C. Rubalcava, S. Safarian *et al.*, "Controlling a below-the-elbow prosthetic arm using the infinity foot controller," *Prosthesis*, vol. 5, no. 4, pp. 1206–1231, 2023.
- [17] X. Hu, J. Wang, W. Gao, C. Yu, and Y. Shi, "Footui: Assisting people with upper body motor impairments to use smartphones with foot gestures on the bed," in *CHI*, 2021, pp. 436:1–436:7.
- [18] C. Zhu, L. Luo, J. Mai, and Q. Wang, "Recognizing continuous multiple degrees of freedom foot movements with inertial sensors," *IEEE Trans. Neural Syst. Rehabilitation Eng.*, vol. 30, pp. 431–440, 2022.
- [19] T. Bikias, D. Iakovakis, S. Hadjidimitriou, V. S. Charisis, and L. J. Hadjileontiadis, "Deepfog: An imu-based detection of freezing of gait episodes in parkinson's disease patients via deep learning," *Front. Robot. AI*, vol. 8, p. 537384, 2021.
- [20] K. Lee, J.-H. Kim, H. Hong, Y. Jeong, H. Ryu, H. Kim, and S.-U. Lee, "Deep learning model for classifying shoulder pain rehabilitation exercises using imu sensor," *J. neuroeng*, vol. 21, no. 1, p. 42, 2024.
- [21] I. E. Jaramillo, J. G. Jeong, P. R. Lopez, C. Lee, D. Kang, T. Ha, J. Oh, H. Jung, J. H. Lee, W. H. Lee, and T. Kim, "Real-time human activity recognition with IMU and encoder sensors in wearable exoskeleton robot via deep learning networks," *Sensors*, vol. 22, no. 24, p. 9690, 2022.
- [22] J. Anlauff, T. Kim, and J. R. Cooperstock, "Feel-a-bump: Haptic feedback for foot-based angular menu selection," in *IEEE Haptics*, K. J. Kuchenbecker, G. J. Gerling, and Y. Visell, Eds., 2018, pp. 175–179.
- [23] G. V. Tchane Djogdom, M. J.-D. Otis, and R. Meziane, "Dynamic time warping-based feature selection method for foot gesture cobot operation mode selection," *Int. J. Adv. Manuf. Technol.*, vol. 126, no. 9, pp. 4521–4541, 2023.
- [24] A. Dahiya, D. Wadhwa, R. Katti, and L. G. Occhipinti, "Efficient hand gesture recognition using artificial intelligence and imu based wearable device," *IEEE Sens. Lett.*, 2024.
- [25] T.-C. Chang, Y.-C. Wu, C.-C. Han, and C.-S. Chang, "Real-time arm motion tracking and hand gesture recognition based on a single inertial measurement unit," in *IOTSMS*, 2024, pp. 44–49.
- [26] O. Makaussov, M. Krassavin, M. Zhabinets, and S. Fazli, "A low-cost, imu-based real-time on device gesture recognition glove," in *SMC*, 2020, pp. 3346–3351.
- [27] D. P. Kingma and J. Ba, "Adam: A method for stochastic optimization," in *ICLR*, 2015.
- [28] B. K. Iwana and S. Uchida, "Time series classification using local distance-based features in multi-modal fusion networks," *Pattern Recognit.*, vol. 97, p. 107024, 2020.
- [29] Y. Wang and H. Ma, "Real-time continuous gesture recognition with wireless wearable IMU sensors," in *Healthcom*, 2018, pp. 1–6.
- [30] M. Brossard, S. Bonnabel, and A. Barrau, "Denoising IMU gyroscopes with deep learning for open-loop attitude estimation," *IEEE Robotics Autom. Lett.*, vol. 5, no. 3, pp. 4796–4803, 2020.
- [31] M. Elad, B. Kowar, and G. Vaksman, "Image denoising: The deep learning revolution and beyond - A survey paper," *SIAM J. Imaging Sci.*, vol. 16, no. 3, pp. 1594–1654, 2023.
- [32] F. M. Carlucci, L. Porzi, B. Caputo, E. Ricci, and S. R. Bulò, "Autodial: Automatic domain alignment layers," in *IEEE ICCV*, 2017, pp. 5077–5085.
- [33] S. Abbaspourazad, O. Elachqar, A. C. Miller, S. Emrani, U. Nallasamy, and I. Shapiro, "Large-scale training of foundation models for wearable biosignals," in *ICLR*, 2024.
- [34] R. Feliuss, M. Punt, M. Geerars, N. Wouda, R. Rutgers, S. Bruijn, S. David, and J. van Dieën, "Exploring unsupervised feature extraction of imu-based gait data in stroke rehabilitation using a variational autoencoder," *PLoS One*, vol. 19, no. 10, p. e0304558, 2024.
- [35] L. Resnik, L. Adams, M. Borgia, J. Delikat, R. Disla, C. Ebner, and L. S. Walters, "Development and evaluation of the activities measure for upper limb amputees," *Arch. Phys. Med. Rehabil.*, vol. 94, no. 3, pp. 488–494, 2013.